

# On the diffusive anomalies in a long-range Hamiltonian system

Luis G. Moyano

Centro Brasileiro de Pesquisas Físicas - Rua Xavier Sigaud 150, 22290-180, Rio de Janeiro, Brazil

Celia Anteneodo

Departamento de Física, Pontifícia Universidade Católica do Rio de Janeiro, CP 38071, 22452-970, Rio de Janeiro, Brazil

We scrutinize the anomalies in diffusion observed in an extended long-range system of classical rotors, the HMF model. Under suitable preparation, the system falls into long-lived quasi-stationary states presenting super-diffusion of rotor phases. We investigate the diffusive motion of phases by monitoring the evolution of their probability density function for large system sizes. These densities are shown to be of the q-Gaussian form,  $P(x) \sim (1 + (q-1)|x|^q)^{-1/(q-1)}$ , with parameter  $q$  increasing with time before reaching a steady value  $q^* = 3/2$ . From this perspective, we also discuss the relaxation to equilibrium and show that diffusive motion in quasi-stationary trajectories strongly depends on system size.

PACS numbers: 05.20.-y, 05.60.Cd, 05.90.+m

## I. INTRODUCTION

Systems with long-range interactions constitute a very appealing subject of research as they display a variety of dynamic and thermodynamic features very different from those of short-range systems treated in the textbooks (see [1] for a review on the subject). Moreover, in recent years, the study of long-range models have raised a renewed interest due to the possible applicability of "Nonextensive Statistics" [2] to such systems.

A very simple model that offers the possibility of investigating many issues related to long-range interactions is the Hamiltonian Mean-Field (HMF) model [3]. It consists of  $N$  planar classical spins interacting through infinite-range couplings. The dynamical variables of each spin  $i$  are a phase angle  $\phi_i$  and its conjugate momentum  $p_i$  whose evolution derives from the Hamiltonian

$$H = \frac{1}{2} \sum_{i=1}^N p_i^2 + \frac{1}{2N} \sum_{i,j=1}^N [\cos(\phi_i - \phi_j)] \quad (1)$$

This model can be seen as a variant of the XY ferromagnet, equipped with a natural Newtonian dynamics. Although the range of interactions is infinite, the HMF has been shown to behave in many aspects qualitatively like its long (finite)-range analogs [4]. Then, despite its simplicity, it reflects features of real systems with long-range forces such as galaxies and charged plasmas [1].

Its equilibrium thermodynamics can be solved in the canonical ensemble. It presents a ferromagnetic second-order phase transition, from a low energy clustered phase to a high energy homogeneous one that occurs at critical temperature  $T_c = 0.5$  (i.e., critical specific energy  $\epsilon_c = 0.75$ ) [3]. However, concerning the microscopic dynamics, the system may get trapped into trajectories over which averaged quantities remain constant during long periods of time with values different from those expected at equilibrium. For instance, for water-bag initial conditions (i.e.,  $\phi_i = 0.8i$ , and  $p_i$  randomly taken from a uniform distribution), a quasi-stationary (QS) state appears

at energies close below  $\epsilon_c$  [5]. In a QS state, the temperature (twice the specific mean kinetic energy) is almost constant in time and lower than the canonical value to which it eventually relaxes. However, the duration of QS states increases with the system size  $N$ , indicating that these states are indeed relevant in the  $(N \rightarrow \infty)$  thermodynamic limit (TL).

Several other peculiar features have been found for out-of-equilibrium initial conditions, e.g., negative specific heat [3], non-Maxwellian momentum distributions [5], glassy dynamics [6], aging [7, 8], anomalous diffusion [9], and others. In particular, anomalous diffusion has been initially associated to quasi-stationarity [9] and later to the (non-stationary) relaxation to equilibrium [10]. Moreover, controversies about the characterization of these states have arisen [11], remaining still aspects of the anomaly in diffusion to be investigated. In this work we report new results on anomalous diffusion and relaxation to equilibrium, focusing on the dependence on system size.

## II. RESULTS

The equations of motion derived from Eq. (1)

$$\begin{aligned} \dot{\phi}_i &= p_i; & \text{for } 1 \leq i \leq N \\ \dot{p}_i &= M_y \cos \phi_i - M_x \sin \phi_i; \end{aligned} \quad (2)$$

where  $M = \frac{1}{N} \sum_{j=1}^N (\cos \phi_j; \sin \phi_j)$  is the magnetization, were solved by means of a symplectic fourth order algorithm [12]. Integrations were performed for fixed  $\epsilon = 0.69$ , for which quasi-stationary effects are more pronounced. Moreover, in the continuum limit, QS trajectories at energies around that value are stable stationary solutions of Vlasov equation [13, 14]. We considered two classes of initial conditions. One of them is a slight variation of water-bag initial conditions normally used in the literature: setting  $\phi_i = 0$  for  $i = 1; \dots; N$ , and regularly valued momenta (instead of random ones) with the

addition of a small noise to allow for statistical realizations. This type of initial condition preserves the main features of random water-bag ones but the QS temperature  $T_{QS}$  is even lower and the duration of the QS regime is longer, in some way mimicking larger systems [13]. We also performed simulations for equilibrium (EQ) initial conditions: waiting an appropriate transient after picking spatial coordinates and momenta from Boltzmann-Gibbs statistics.

Integration of Eqs. (2) yields phases in  $(\theta; \dot{\theta})$ . Then, we measured the histograms of phases at different times, accumulating the data over several realizations to improve the statistics. Actually, the dynamics depends on the phases modulo  $2\pi$ , since they enter into the equations of motion as argument of sine and cosine functions. However, the statistics of unbounded phases is relevant as it reflects features of momentum space, which displays anomalies such as non-Maxwellian distributions [5] and two-time correlations signaling "aging" effects [8]. For instance, a simple mathematical relationship exists between the standard deviation of angles and velocity correlations [10].

For low energies, phases are confined, while for sufficiently large energies, they evolve in diffusive motion. In Fig. 1 we show the properly scaled probability density functions (PDFs) of rotor phases at different times, for fixed size  $N = 1000$  and energy per particle  $\epsilon = 0.69$ , starting from water-bag initial conditions. After transient stages, numerical histograms can be very well described in the whole range by the q-Gaussian function [2]

$$P(\theta) = A [1 + (q-1)(\theta/\sigma)^2]^{-1/q}; \quad (3)$$

where  $A$  is a normalization factor and  $\sigma$  a positive constant. This function includes the standard Gaussian when  $q=1$  and presents power-law tails for  $q > 1$ . Recalling that the PDF (3) has variance  $\sigma^2 = \sigma^2(5-3q)$ , for  $q < 5/3$ , and considering normalized angles  $\theta/\sigma = \theta$ , then Eq. (3) can be written as the uni-parametric function

$$P_q(\theta) = A_q [1 + \frac{q-1}{5-3q} \theta^2]^{-1/q}; \quad (4)$$

with  $A_q = \frac{q}{(5-3q)} \frac{1}{(1+(q-1)\theta^2)}$ . At each instant  $t$  of the dynamics,  $\sigma^2$  is computed as

$$\sigma^2(t) = h(\langle \theta^2 \rangle_t); \quad (5)$$

where  $\langle \cdot \rangle_t$  denotes average over the  $N$  rotors and over different realizations of the dynamics at time  $t$ . As far as we know, this is the first time that pure q-Gaussian PDFs arising from a Hamiltonian dynamics are detected.

In Fig. 2d, the evolution of  $q$  for different  $N$  is displayed, including the fitting values used in Fig. 1 for  $N = 1000$ . Parameter  $q$  increases up to a steady value in

the long-time limit, that for all  $N$  falls within the range  $q \in [1.51, 0.02]$ . In the same figure, we also exhibit the temporal evolution of temperature  $T(t) = \frac{1}{N} \sum_i p_i^2$  (Fig. 2.a) and dispersion  $\sigma^2(t)$  (Fig. 2.b), in order to establish a parallel between the different stages of the relevant quantities. Instead of single runs, averaged quantities are presented. Since they are much less noisy, they allow the representation of several curves in the same plot without distorting the main features observed in individual runs. We can see that  $q$  attains a steady value approximately when the QS-EQ transition is completed. In Fig. 3 the same data are presented for rescaled times.

The PDFs of rotor phases, for  $N = 500$ , and  $\epsilon = 0.69$ , but starting from an equilibrium configuration are shown in Fig. 4. In this case, histograms present pronounced shoulders that persist for long times and can not be well described by q-Gaussian functions. However, as time goes by, the shoulders shift away from the center and the histograms tend to a q-Gaussian function, with  $q$  going to  $q = 3/2$  from above in the long-time limit.

Then, starting both from equilibrium and out-of-equilibrium (water-bag) configurations, initially confined densities of phases develop power-law tails and adopt q-Gaussian forms.

Diffusion of spatial coordinates may be characterized by the average squared displacement  $\langle \theta^2(t) \rangle$  of the angles as defined by Eq. (5). In the one-dimensional generalized Einstein relation

$$\langle \theta^2(t) \rangle = 2D t; \quad (6)$$

where  $D$  is the diffusion constant, the case  $\epsilon = 1$  corre-

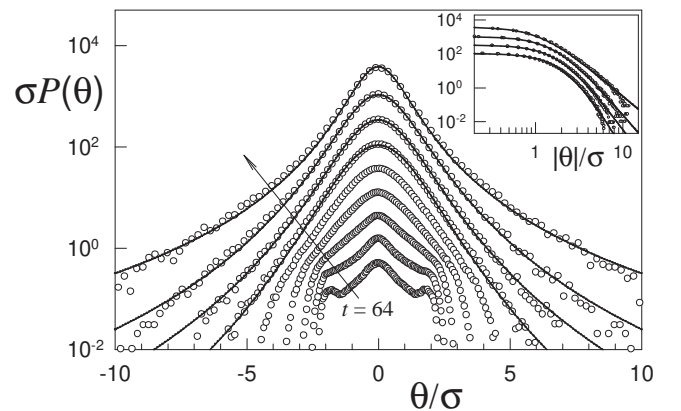


FIG. 1: Histograms of rotor phases at different instants of the dynamics (symbols). Simulations for  $N = 1000$  were performed starting from regular water-bag initial conditions at  $\epsilon = 0.69$  (conditions leading to QS states). Countings were accumulated over 100 realizations, at times  $t_k = 2^k$ , with  $k = 6; 8; \dots; 14$ , growing in the direction of the arrow up to  $t = 16384$ . Solid lines correspond to q-Gaussian fittings. Histograms were shifted for visualization. Inset: log-log representation of the fitted data.

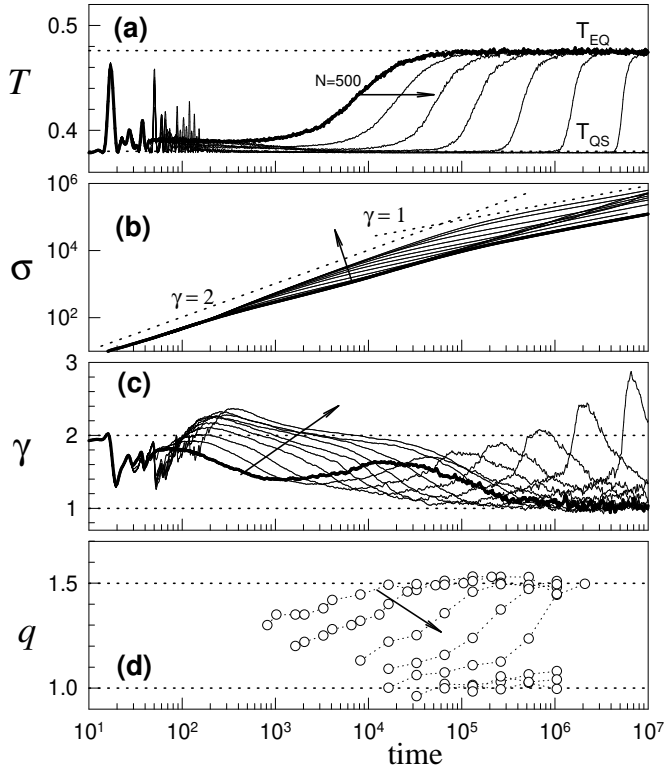


FIG. 2: Averaged time series of (a) temperature  $T$ , (b) deviation  $\sigma$ , (c) diffusion exponent  $\gamma$  and (d) parameter  $q$ , for  $\mu = 0.69$  and different values of  $N$  ( $N = 500 \cdot 2^k$ , with  $k = 0; \dots; 9$ ). Bold lines correspond to  $N = 500$ , as reference, and  $N$  increases in the direction of the arrows up to  $N = 256000$ . Averages were taken over  $2.56 \cdot 10^5 = N$  realizations, starting from a waterbag configuration at  $t = 0$ . In panel (d), the fitting error is approx. 0.03. Dotted lines are drawn as references. In (a), they correspond to temperatures at equilibrium ( $T_{EQ} = 0.476$ ) and at QS states in the TL ( $T_{QS} = 0.38$ ). In (b), to ballistic motion ( $\gamma = 2$ ) and normal diffusion ( $\gamma = 1$ ).

responds to normal diffusion,  $\gamma < 1$  to sub-diffusion and super-diffusion occurs for  $\gamma > 1$ . The evolution of  $\gamma$  is shown in Figs. 2b and 5b, for water-bag and equilibrium initial preparations, respectively. In order to detect different regimes, it is useful to obtain an instantaneous exponent  $\gamma$  as a function of time by taking the logarithm in both sides of Eq. (6) and differentiating with respect to  $\ln t$ :

$$\gamma(t) = \frac{d(\ln \sigma^2)}{d(\ln t)} : \quad (7)$$

The outcome of this procedure can be seen in Fig. 2c for water bag initial conditions. The same analysis for system prepared in an equilibrated configuration is presented in Fig. 5c.

For the latter class of initial conditions, phase motion

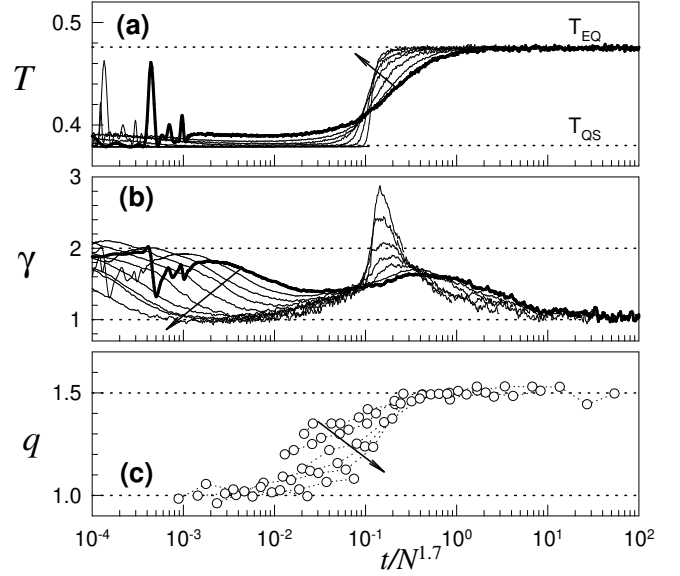


FIG. 3: Averaged time series of (a) temperature  $T$ , (b) local exponent  $\gamma$  and parameter  $q$  (symbols), as a function of  $t/N^{1.7}$ . Data are the same presented in Fig. 2.

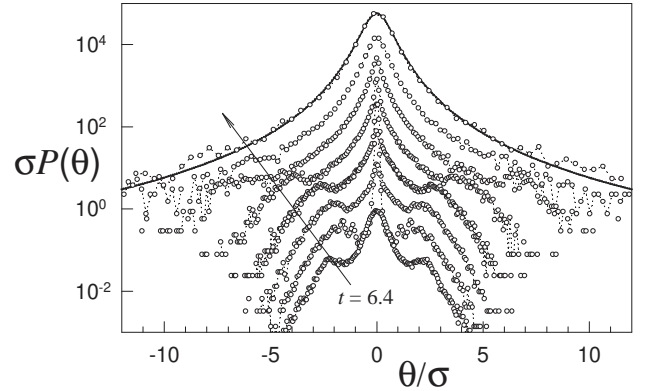


FIG. 4: Histograms of rotor phases at different instants of the dynamics (symbols). Simulations were performed for  $N = 500$  and  $\mu = 0.69$ , starting from an equilibrated initial condition. Countings were accumulated over 200 realizations, at times  $t_k = 0.1 \cdot 4^k$ ,  $k = 3; 4; \dots; 10$ , growing in the direction of the arrow up to  $t = 1.05 \cdot 10^5$ . The q-Gaussian function with  $q = 1.53$  was plotted for comparison (solid line). Histograms were shifted for visualization.

is ballistic ( $\gamma = 2$ ) at short time scales in which rotors move almost freely, while phases display normal diffusion ( $\gamma = 1$ ) in the long-time limit, as shown in Fig. 5 (see also [10]). The crossover between both behaviors shifts to larger times as  $N$  increases. We observed this same pattern of behaviors also at supercritical energies ( $\mu = 5$ ),

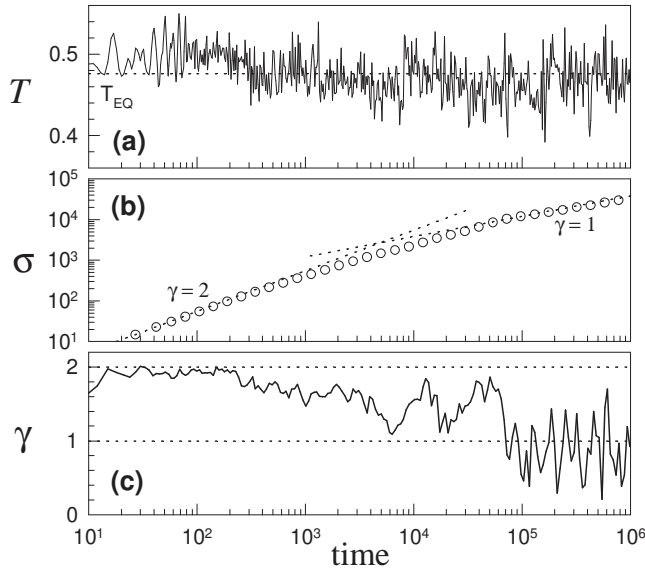


FIG. 5: Time series of (a) temperature  $T$ , (b) deviation  $\sigma$  and (c) diffusion exponent  $\gamma$ , for  $N = 500$  and  $\nu = 0.69$ . At  $t = 0$ , the system is in an equilibrium configuration. The outcome of a single run is exhibited.

although in Ref. [9] only the ballistic regime was reported since normal diffusion settles at times longer than those analyzed in that work.

For water-bag initial conditions, both ballistic and normal regimes are also observed for short and long times, respectively. However, in this case, the crossover is more complex (see Figs. 2(c) and 3(c)): Exponent  $\gamma$  varies non-monotonously taking super-diffusive values and it does not present a well defined plateau as temperature does. For this intermediate stage, super-diffusion has been reported before and attributed to a kind of Levy-walk mechanism, yielding a succession of free walks and trapping events[9]. Also, it has been interpreted from a topological perspective[15].

The main features one observes in the profile of local exponent  $\gamma$  vs. time can be summarized as follows: (i) In a first stage,  $\gamma$  takes a maximum value that remains close to  $\gamma = 2$ , corresponding to ballistic motion. This stage occurs at the beginning of the QS regime and its duration increases with  $N$ . (ii) Then  $\gamma$  reaches a minimum value that as  $N$  increases falls within the QS range. Also as  $N$  increases, the valley broadens and  $\gamma$  attens, and the minimum value tends to unity (see Fig. 3). Thus, anomalous diffusion in QS states is a finite-size effect, as already pointed out by Yamaguchi from a different perspective and for a different initial preparation [10]. (iii) Another maximum appears in correspondence to the rapid relax-

ation from QS to EQ. The maximum value grows with  $N$ , largely exceeding the value  $\gamma = 2$ . But the peak narrows, hence it lasts less. This peak corresponds approximately to the inflexion point in the time evolution of temperature (Figs. 2 and 3), whose slope increases with  $N$ . In fact, in the QS  $\rightarrow$  EQ relaxation, the rapid increase of  $T$  (kinetic energy) leads to an accelerated increase of the phases in average. (iv) In the final stage,  $\gamma$  relaxes asymptotically to unity, indicating normal diffusion at very long times.

### III. DISCUSSION AND REMARKS

From the analysis of  $\gamma$ , one concludes that diffusive motion in QS trajectories strongly depends on the system size. In the  $\gamma$  vs.  $t$  profile, as  $N$  increases, the neighborhood of the first minimum (that becomes contained in the QS range defined by  $T$ ) attens, defining a quasi-stationary value of  $\gamma$ . This steady value goes to one in the TL. All these features are neatly observed in Fig. 3. Then, diffusion in QS states becomes of the normal type in that limit. For the whole time span, non-trivial values of  $\gamma$  occur in the TL only at non-stationary (nor quasi-stationary) stages, consistently with observations by Yamaguchi[10].

Moreover, the spreading of initially confined phases develops power-law tails. For QS trajectories, histograms adopt a q-Gaussian form with  $q$  increasing up to a steady value  $q \approx 3=2$ . A similar steady value is also attained asymptotically when starting at equilibrium. For both classes of initial conditions, stabilization of parameter  $q$  is reached only when equilibrium holds and  $\gamma$  attains the steady value corresponding to normal diffusion.

Let us note that Levy densities present power-law tails with exponents restricted to a given interval (yielding divergent second moment) that in terms of parameter  $q$  corresponds to  $q > 5=3$ , therefore, not including the observed values. While the generalization of the standard diffusion equation with fractional spatial derivatives leads to Levy functions, the non-linear generalization  $\partial_t P(x;t) = D \partial_{xx} [P(x;t)]^q$ , with constant  $D$  and  $q$ , has q-Gaussian functions as long-time solutions[16]. The non-linear equation yields anomalous diffusion of the correlated type with exponent  $\gamma = 2=(3-q)$ . In our case, power-law tails also develop. Although they are characterized by  $q$  changing with time, the fact that it attains a steady value suggests that the spreading of phases may be ruled by an akin non-linear process. In such case, effective parameters are  $q_{eff} \approx 1.5$  and  $\gamma_{eff} \approx 1.33$ . However, this issue as well as a possible connection with Nonextensive Statistics should be further investigated.

### Acknowledgments

We are grateful to C. Tsalis for fruitful discussions. L.G.M. acknowledges the kind hospitality at Santa Fe Institute where part of this work was made. We ac-

knowledge Brazilian agency CNPq for partial financial support.

- 
- [1] T. Dauxois, S. Ruo, E. Arimondo and M. Wilkens, eds., *Dynamics and Thermodynamics of Systems with Long Range Interactions*, Lecture Notes in Physics Vol. 602, Springer (2002), and references therein.
- [2] C. Tsalis, *J. Stat. Phys.* 52, 479 (1988); *Nonextensive Mechanics and Thermodynamics*, edited by S. Abe and Y. Okamoto, Lecture Notes in Physics Vol. 560 (Springer, Berlin, 2001); in *Non-Extensive Entropy-Interdisciplinary Applications*, edited by M. Gell-Mann and C. Tsalis, (Oxford University Press, Oxford, 2004).
- [3] M. Antoni and S. Ruo, *Phys. Rev. E* 52, 2361 (1995).
- [4] C. Anteneodo and C. Tsalis, *Phys. Rev. Lett.* 80, 5313 (1998); F. Tamari and C. Anteneodo, *Phys. Rev. Lett.* 84, 208 (2000); C. Anteneodo and R. O. Vallejos, *Phys. Rev. E* 65, 016210 (2001); M. C. Firpo and S. Ruo, *J. Phys. A* 34, L511 (2001); A. Giansanti, D. Moroni and A. Campa, *Chaos, Sol. & Frac.* 13, 407 (2002); B. J. C. Cabral and C. Tsalis, *Phys. Rev. E* 66, 065101 (R) (2002); R. O. Vallejos and C. Anteneodo, *Physica A* 340, 178 (2004).
- [5] V. Latora, A. Rapisarda, and C. Tsalis, *Phys. Rev. E* 64, 056134 (2001); V. Latora, A. Rapisarda, and C. Tsalis, *Physica A* 305, 129 (2002).
- [6] A. Pluchino, V. Latora and A. Rapisarda, *Physica A* 340, 187 (2004); *Phys. Rev. E* 69, 056113 (2004).
- [7] M. A. Montemurro, F. A. Tamari and C. Anteneodo, *Phys. Rev. E* 67, 031106 (2003).
- [8] A. Pluchino, V. Latora, and A. Rapisarda, *Physica D* 193, 315 (2004).
- [9] V. Latora, A. Rapisarda and S. Ruo, *Phys. Rev. Lett.* 83, 2104 (1999).
- [10] Y. Yamaguchi, *Phys. Rev. E* 68, 066210 (2003).
- [11] D. H. Zanette and M. A. Montemurro, *Phys. Rev. E* 67, 031105 (2003), C. Tsalis, *Physica D* 193, 3 (2004), A. Pluchino, V. Latora and A. Rapisarda, *Physica D* 193, 315 (2004).
- [12] F. Neri, *Lie algebras and canonical integration*, Department of Physics, University of Maryland, preprint (1988); H. Yoshida, *Phys. Lett. A* 150, 262 (1990).
- [13] C. Anteneodo, and R. O. Vallejos, *Physica A* 344, 383 (2004).
- [14] Y. Yamaguchi, J. Barre, F. Bouchet, T. Dauxois, and S. Ruo, *Physica A* 337, 36 (2004).
- [15] F. A. Tamari, G. M. Agliano, D. A. Stariob, and C. Anteneodo, *Phys. Rev. E* 71, 036148 (2005).
- [16] A. R. Plastino and A. Plastino, *Physica A* 222, 347 (1995); C. Tsalis and D. J. Bukman, *Phys. Rev. E* 54, R2197 (1996); L. A. Peletier in *Applications of nonlinear analysis in the physical sciences* (Pitman, Massachusetts, 1981).